



Triplet to singlet transition induced low efficiency roll-off in green phosphorescent organic light-emitting diodes

Zisheng Su^{a,b}, Wenlian Li^{a,*}, Bei Chu^{a,*}, Shuanghong Wu^{a,b}

^a Key Laboratory of Excited State Processes, Changchun Institute of Optics, Fine Mechanics and Physics, Chinese Academy of Sciences, Changchun 130033, People's Republic of China

^b Graduate School of Chinese Academy of Sciences, Beijing 100039, People's Republic of China

ARTICLE INFO

Article history:

Received 10 March 2010

Received in revised form 24 September 2010

Accepted 1 December 2010

Available online 8 December 2010

Keywords:

Phosphorescent organic light-emitting diodes

Efficiency roll-off

Energy transfer

ABSTRACT

Phosphorescent organic light-emitting diodes (PHOLEDs) with an emitting layer of 4,4'-N,N'-dicarbazole-biphenyl codoped with phosphor *fac*-tri(phenylpyridine)iridium(III) [Ir(ppy)₃] and fluorophore N,N'-dimethyl-quinacridone (DMQA) are investigated. Predominant emission from DMQA due to the efficient energy transfer from Ir(ppy)₃ to DMQA is observed. Such an energy transfer results in the transition of Ir(ppy)₃ triplet to DMQA singlet, which reduces the Ir(ppy)₃ exciton lifetime and hence suppresses the triplet–triplet annihilation and triplet–polaron annihilation of Ir(ppy)₃ excitons, leading to dramatical reduction of the efficiency roll-off of the PHOLEDs. This transition of triplet to singlet strategy provides a method to improve the efficiency roll-off of the PHOLEDs.

© 2010 Elsevier B.V. All rights reserved.

1. Introduction

Since the demonstration of the double-layer devices in 1987, organic light-emitting diodes (OLEDs) have been attracting more and more attentions [1]. By doping fluorescent [2] or phosphorescent [3] emitting species into the emitting layer (EML), the electroluminescent (EL) performance of the OLEDs were significantly improved. Statistically, the excitons are formed in the ratio of one singlet to three triplets by electrical injection [4]. The emission of the fluorescent OLEDs results from the singlet excitons radiation, suggesting a maximum internal quantum efficiency of only 25%. In contrast, the phosphorescent OLEDs (PHOLEDs) can harvest both the singlet and triplet excitons, leading to the potential for reaching a maximum internal quantum efficiency of 100% [5]. In recent years, PHOLEDs have drawn a lot of interest due to their potential applications for high efficiency full color displays and next generation lighting sources [6–9]. However, the PHOLEDs suffer from a dramatically decrease in EL efficiency at high current density, which is predominantly ascribed to the triplet–triplet annihilation (TTA) and triplet–polaron annihilation (TPA) due to the long radiative lifetime of the triplet excitons [10,11]. Many methods have been proposed to reduce the efficiency roll-off of the PHOLEDs, such as using double EML structure [12,13], mixed host devices [14], high triplet energy hole transport materials [15], and fluorescence-interlayer-phosphorescence structure [16] to broaden the recombination zone and confine excitons in the EML, using exciton undoped interlayer in the EML to eliminate aggregation the

emitter dopant [17,18], and using high mobility electron transport material to balance the injection of the carriers [19].

Although the fluorescent OLEDs present low efficiency, their low efficiency roll-off character is attractive. While the PHOLEDs give high efficiency, they bring up a disgusting efficiency roll-off. Thus devices combining the advantages of the high efficiency of PHOLEDs and the low efficiency roll-off of fluorescent OLEDs are particularly desirable. The fluorophore and the phosphor emitters codoped strategy, where the triplet excitons can be formed in the phosphor followed by energy transfer to the fluorophore singlets and eventually radiated, may offer a technique to realize such a combination [20–23]. This codoped strategy has been adopted to improve the performance of the fluorescent OLEDs, where the energy of the phosphor triplet is usually much higher than that of the fluorophore singlet, which leads to large exchange energy loss during the energy transfer process. N,N'-dimethyl-quinacridone (DMQA) and *fac*-tri(phenylpyridine)iridium(III) [Ir(ppy)₃] are the typical green fluorophore and phosphor with singlet and triplet energy of about 2.34 and 2.43 eV, respectively [24,25]. In this letter, DMQA and Ir(ppy)₃ are codoped into 4,4'-N,N'-dicarbazole-biphenyl (CBP) acted as the EML. Efficient energy transfer from Ir(ppy)₃ triplet to DMQA singlet is demonstrated. And the energy transfer leads to the transition of the Ir(ppy)₃ triplet to the DMQA singlet. Such a transition results in a dramatically reduced exciton lifetime of Ir(ppy)₃ and hence the efficiency roll-off of the devices.

2. Experimental details

The devices have a structure of indium tin oxide (ITO)/4,4',4''-tris[2-naphthyl(phenyl)amino]triphenylamine (2-TNATA) (5 nm)/N,N'-

* Corresponding authors. Tel./fax: +86 431 86176345.

E-mail addresses: wllioel@yahoo.com.cn (W. Li), beichu@163.com (B. Chu).

diphenyl-N,N'-bis(1-naphthyl)-(1,1'-benzidine)-4,4'-diamine (NPB) (40 nm)/EML (30 nm)/4,7-diphenyl-1,10-phenanthroline (Bphen) (10 nm)/tris(8-hydroxyquinoline)aluminum (Alq₃) (20 nm)/LiF (0.5 nm)/Al (100 nm). Where, 2-TNATA, NPB, Bphen, and Alq₃ act as hole-injection layer, hole-transporting layer, exciton-blocking layer, and electron-transporting layer, respectively. The EML comprised of CBP doped with different concentrations of DMQA and Ir(ppy)₃, and for reference the Ir(ppy)₃ monodoped device with optimized doping concentration of 6 wt.% was also fabricated. Organic layers were deposited onto a precleaned ITO glass substrate with a sheet resistance of 25 Ω/sq by thermal evaporation in vacuum chamber at 3 × 10⁻⁴ Pa, followed by a LiF buffer layer and an Al cathode in the same vacuum run. The deposition rates and thickness of the layers were monitored in situ using oscillating quartz monitors. The evaporating rates were kept at 0.5–1 Å/s for organic layers and LiF layer and 10 Å/s for Al cathode, respectively. Absorption spectrum was measured with a Shimadzu UV-3101 spectrophotometer. Photoluminescent (PL) spectra were measured with a Hitachi F-4500 fluorescence spectrophotometer. EL spectra of the devices were measured with a CCD spectrometer. Luminance–current–voltage (L–I–V) characteristics were measured with a Keithley 2400 power supply combined with a spot photometer and were recorded simultaneously with measurements. The external quantum efficiency of the devices was calculated from their EL spectra and L–I–V characteristics. PL transition decay was measured with a FL920-fluorescence lifetime spectrometer (Edinburgh instrument), and the excitation source was an nF900 ns flash lamp. All the measurements were carried out at room temperature under ambient condition.

3. Results and discussions

Fig. 1 shows the normalized absorption spectrum of DMQA and the PL spectra of CBP and Ir(ppy)₃ in CH₂Cl₂ solutions. It can be found that the absorption spectrum of DMQA has large overlaps with the PL spectra of CBP and Ir(ppy)₃, indicating the likelihood of efficient energy transfer from both CBP and Ir(ppy)₃ to DMQA.

To optimize the doping concentration of DMQA, devices monodoped with DMQA were fabricated. Fig. 2 presents the normalized EL spectra of the devices. Two emission bands located at about 440 and 530 nm in the EL spectra are observed, which are attributed to the emission of NPB and DMQA, respectively. The emission of NPB may come from the energy transfer from CBP due to the saturated emission of DMQA and/or the recombination zone located in the NPB/CBP interface in the low DMQA doped devices. This NPB emission disappears with the increase of the DMQA concentration. In all devices the emission of CBP is not observed, indicating that an efficient energy transfer from CBP to DMQA.

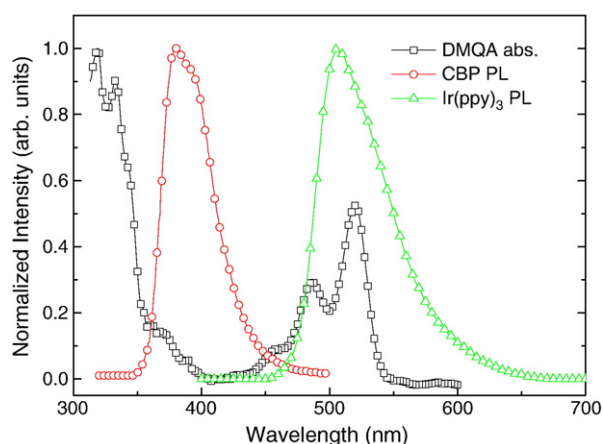


Fig. 1. Absorption spectrum and PL spectra of DMQA, CBP and Ir(ppy)₃ in CH₂Cl₂ solutions.

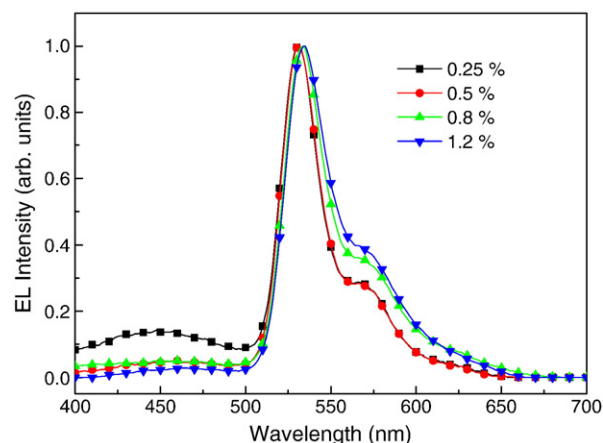


Fig. 2. EL spectra of the DMQA monodoped devices with different concentrations.

Table 1 summarizes the EL performance of the DMQA monodoped devices. The efficiency increases with the doping concentration of DMQA, and a maximum current efficiency of 7.08 cd/A, a maximum power efficiency of 4.03 lm/W, and a maximum external quantum efficiency of 1.85% are obtained with DMQA doping concentration of 0.50 wt.%. These values are comparable with the DMQA doped Alq₃ devices reported elsewhere [24]. The efficiency decreases significantly with further increased DMQA doping concentration due to the concentration quenching. In terms of the EL performance, DMQA concentrations of 0.25 wt.% and 0.50 wt.% were selected to construct the codoped devices.

Fig. 3 plots the normalized EL spectra of the 0.25 wt.% DMQA and 12 wt.% Ir(ppy)₃ codoped device at different applied voltage. The EL spectrum shows a weak dependent on the applied voltage. The primary emission at 530 nm with the shoulder at about 570 nm comes from DMQA, while another weaker shoulder at about 510 nm results from the emission of Ir(ppy)₃. And all the EL spectra of the devices codoped with DMQA and Ir(ppy)₃ present similar low emission intensity of Ir(ppy)₃ compared to DMQA (not shown here). We have tried to fit the EL spectra of the codoped device by the Ir(ppy)₃ and DMQA EL spectra. It is found that the fitted curve has a large deviation from the actual one, which should be attributed to the different mechanisms involved in the monodoped and codoped devices and consequently different emission peaks and sharps. Thus it is difficult to actually calculate the proportion of the Ir(ppy)₃ emission on the whole EL emission. However, it can be found in the EL spectra that the emission intensity at 510 nm is much lower than that at 530 nm, which indicates that the DMQA is the predominant emission component.

The EL performance of the devices doped with different concentrations of DMQA and Ir(ppy)₃ is listed in Table 2. The 6 wt.% Ir(ppy)₃ doped reference device shows a maximum quantum efficiency of 9.33%, and it decreases obviously with the increase of the current density, as shown in Fig. 4. The maximum quantum efficiency of the 0.25 wt.% DMQA based codoped devices is dramatically improved compared with that of the DMQA monodoped device, and the efficiency increases with the doping concentration of Ir(ppy)₃ at first, then decreases as the concentration further increased. More

Table 1
EL performance of the DMQA monodoped devices.

DMQA concentration (wt.%)	Max η_c (cd/A)	Max η_p (lm/W)	Max η_{ext} (%)
0.25	6.06	3.24	1.81
0.50	7.08	4.03	1.85
0.80	4.32	3.38	0.98
1.20	2.11	1.47	0.44

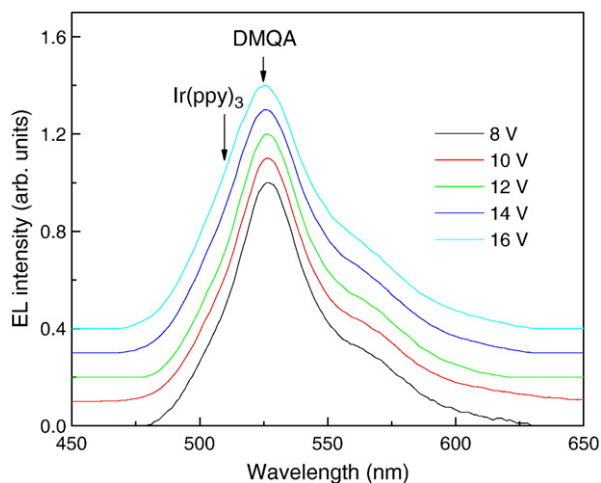


Fig. 3. EL spectra of the 0.25 wt.% DMQA and 12 wt.% Ir(ppy)₃ codoped device at different applied voltage, the arrows denote the emission peaks of Ir(ppy)₃ and DMQA at about 510 and 530 nm, respectively.

interesting, it is found that the efficiency roll-off of the codoped devices is dramatically improved compared with that of the reference device. The quantum efficiency of the reference device at 100 mA/cm² is 4.06%, which is decrease of 56.5% to that of the maximum efficiency. While the efficiency of the 5 wt.%, 8 wt.%, 12 wt.%, and 15 wt.% Ir(ppy)₃ codoped devices at 100 mA/cm are 3.39%, 3.18%, 3.93%, and 1.41%, which are decrease of only 16.7%, 37.0%, 40.6%, and 37.3% to that of their respective maximum efficiency. And the efficiency of the 12 wt.% Ir(ppy)₃ codoped device even exceeds that of the reference device at higher current density. Similarly, the quantum efficiency of the reference device at 10,000 cd/cm² is 4.38%, suggesting a net reduction of 53.1% to that of its maximum efficiency. In contrast, the quantum efficiency of the 5 wt.%, 8 wt.%, 12 wt.%, and 15 wt.% Ir(ppy)₃ codoped devices at 10,000 cd/cm² are 3.50%, 3.34%, 4.24%, and 1.16%, and a relative decrease of only 14.1%, 35.4%, 36.0%, and 48.3% to that of their respective maximum efficiency are obtained. And a higher efficiency is observed for the 12 wt.% Ir(ppy)₃ codoped device compared with the reference device at luminance higher than 20,000 cd/cm². Similar phenomenon was found in the 0.50 wt.% DMQA codoped devices, as listed in Table 2. These findings indicated that the efficiency roll-off of the devices is significantly reduced by codoping the fluorescent material DMQA.

To further understand the photophysics involved, the PL transition decays of the CBP:0.25% DMQA, CBP:12% Ir(ppy)₃, and CBP:12% Ir(ppy)₃:0.25% DMQA films on quartz substrates were investigated, the excitation wavelength was 330 nm and the monitor wavelength were 530, 510, and 510 nm, respectively. The PL spectrum of CBP:Ir(ppy)₃:DMQA exhibits high emission intensity of DMQA at about 530 nm than that of Ir(ppy)₃ at 510 nm, as shown in inset of Fig. 5. The PL

Table 2

External quantum efficiency of the devices doped with different concentrations of DMQA and Ir(ppy)₃.

DMQA concentration (wt.%)	Ir(ppy) ₃ concentration (wt.%)	Max η_{ext} (%)	η_{ext} at 20 mA/cm ² (%)	η_{ext} at 10,000 cd/cm ² (%)
–	6	9.33	4.06	4.38
0.25	5	4.07	3.39	3.50
0.25	8	5.17	3.24	3.34
0.25	12	6.62	3.93	4.24
0.25	15	2.25	1.41	1.16
0.50	3	4.79	2.99	3.09
0.50	5	5.35	3.23	3.37
0.50	8	4.33	2.34	2.25
0.50	12	3.52	2.12	1.97

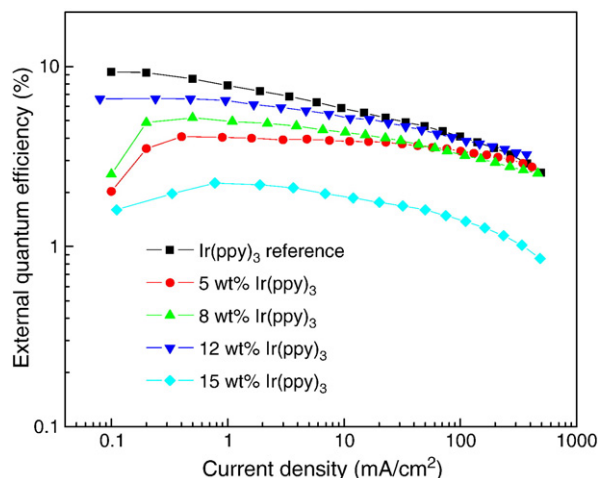


Fig. 4. External quantum efficiency versus current density of the 6% Ir(ppy)₃ doped reference device and the 0.25 wt.% DMQA based codoped devices with different doped concentrations of Ir(ppy)₃.

transition decay of the three films can be fitted by first, second, and third order exponential decay, respectively, according to the method described in reference [26]. Average exciton lifetime of 17, 364, and 78 ns can be extracted from the fitting curves, respectively. It can be found that the decay of the CBP:Ir(ppy)₃:DMQA is more rapid as refer to that of CBP:Ir(ppy)₃. It should be mentioned that the detected decay curve of CBP:DMQA:Ir(ppy)₃ monitored at 510 nm includes the response of DMQA decay signal, and the actual decay of Ir(ppy)₃ should be faster than the curve measured here. Although there are differences of the decays in PL and EL devices [23], the fact that the faster decay in CBP:Ir(ppy)₃:DMQA than in CBP:Ir(ppy)₃ cannot be altered.

Both direct formation of excitons in DMQA under electrical pumping and energy transfer from Ir(ppy)₃ to DMQA, i.e., Ir(ppy)₃ triplet to DMQA singlet and Ir(ppy)₃ triplet to DMQA triplet, could lead to low emission of Ir(ppy)₃ in the EL spectra. The low emission of Ir(ppy)₃ in the EL spectra suggests that the Ir(ppy)₃ emission has a little contribution to the device efficiency. If the direct formation of excitons in DMQA and energy transfer from Ir(ppy)₃ triplet to DMQA triplet were the only mechanisms for the low emission of Ir(ppy)₃ in the EL spectra, the efficiency of the codoped devices should be more

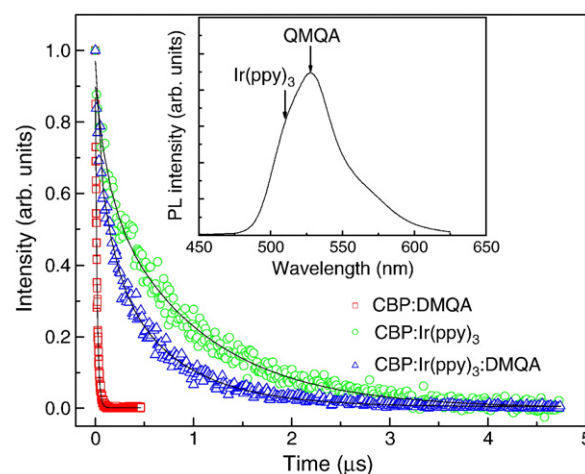


Fig. 5. PL transition decay of the CBP:0.25% DMQA, CBP:12% Ir(ppy)₃, and CBP:12% Ir(ppy)₃:0.25% DMQA films on quartz substrates, the fitting curves of the decays are also shown in the figure. Inset: PL spectrum of CBP:12% Ir(ppy)₃:0.25% DMQA film on quartz substrate excited at 330 nm, the arrows denote the emission peaks of Ir(ppy)₃ and DMQA at about 510 and 530 nm, respectively.

close to that of the DMQA monodoped devices. However, the dramatically increased efficiency of the codoped devices implies that energy transfer from Ir(ppy)₃ triplet to DMQA singlet plays an important role in the codoped devices. Energy transfer from the phosphor triplet to the fluorophore singlet would lead to dramatically reduce of the exciton lifetime of the phosphor and increase of the exciton lifetime of the fluorophore, and the decay of the fluorophore should be governed by that of the phosphor [20]. In view of this, the actual decay of Ir(ppy)₃ in CBP:DMQA:Ir(ppy)₃ should be dramatically faster than the decay of CBP:DMQA:Ir(ppy)₃ measured at 510 nm, that is, the exciton lifetime of Ir(ppy)₃ in CBP:DMQA:Ir(ppy)₃ is dramatically reduced compared to that in CBP:Ir(ppy)₃.

TTA and TPA are considered as the main origins for the efficiency roll-off of PHOLEDs at high current density. The TTA is proportional to the square of triplet exciton density, and the TPA scales with the triplet exciton density. In an OLED under operation conditions, the exciton density is in proportion to the exciton lifetime [11]. As discussed above, the fluorophore and phosphor codoped strategy provides a mechanism for the transition of Ir(ppy)₃ triplet to DMQA singlet, and this transition reduces the Ir(ppy)₃ triplet exciton lifetime. As shown in Fig. 4, the critical current density J_0 defined as the current density when the efficiency decreases to half of the maximum is about 100 mA/cm² for the reference device, and it is about 300 mA/cm² for the 0.25 wt.% DMQA and 12 wt.% Ir(ppy)₃ codoped device. The obvious increase of J_0 can be attributed to the suppression of TTA and TPA due to the shortened exciton lifetime. Although the maximum quantum efficiency of the codoped devices is a little lower than that of the reference device, more interesting revelation one can get from this work is that it provides a method to improve the efficiency roll-off of the PHOLEDs.

4. Conclusions

In summary, the efficiency roll-off of the Ir(ppy)₃ based PHOLEDs is dramatically improved by codoping a fluorophore DMQA into the EML. The improvement can be attributed to the efficient energy transfer from Ir(ppy)₃ to DMQA led transition of Ir(ppy)₃ triplet to DMQA singlet and hence reduces the exciton lifetime of Ir(ppy)₃,

which effectively suppresses the TTA and TPA of Ir(ppy)₃ excitons. This transition of triplet to singlet strategy provides a method to improve the efficiency roll-off of PHOLEDs, and it has the potential application in blue and red PHOLEDs.

References

- [1] C.W. Tang, S.A. VanSkyke, Appl. Phys. Lett. 51 (1987) 913.
- [2] C.W. Tang, S.A. VanSkyke, C.H. Chen, J. Appl. Phys. 65 (1989) 3610.
- [3] M.A. Baldo, D.F. O'Brien, Y. You, A. Shoustikov, S. Sibley, M.E. Thompson, S.R. Forrest, Nature 395 (1998) 151.
- [4] M.A. Baldo, D.F. O'Brien, M.E. Thompson, S.R. Forrest, Phys. Rev. B 60 (1999) 14422.
- [5] C. Adachi, M.A. Baldo, M.E. Thompson, S.R. Forrest, J. Appl. Phys. 90 (2001) 5048.
- [6] B.W. D'Andrade, S.R. Forrest, Adv. Mater. 16 (2004) 1585.
- [7] Y.R. Sun, S.R. Forrest, Org. Electron. 9 (2008) 994.
- [8] S. Reineke, F. Lindner, G. Schwartz, N. Seidler, K. Walzer, B. Lüsslem, K. Leo, Nature 459 (2009) 234.
- [9] M.H. Ho, B. Balaganesan, T.Y. Chu, T.M. Chen, C.H. Chen, Thin Solid Films 517 (2008) 943.
- [10] M.A. Baldo, C. Adachi, S.R. Forrest, Phys. Rev. B 62 (2000) 10967.
- [11] S. Reineke, K. Walzer, K. Leo, Phys. Rev. B 75 (2007) 125328.
- [12] J.W. Kang, S.H. Lee, H.D. Park, W.I. Jeong, K.M. Yoo, Y.S. Park, J.J. Kim, Appl. Phys. Lett. 90 (2007) 223508.
- [13] W.S. Jeon, T.J. Park, S.Y. Kim, R. Pode, J. Jang, J.H. Kwon, Appl. Phys. Lett. 93 (2008) 063303.
- [14] S.H. Kim, J. Jang, K.S. Yook, J.Y. Lee, Appl. Phys. Lett. 92 (2008) 023513.
- [15] S.O. Jeon, K.S. Yook, C.W. Joo, J.Y. Lee, K.Y. Ko, J.Y. Park, Y.G. Baek, Appl. Phys. Lett. 93 (2008) 063306.
- [16] T. Zheng, W.C.H. Choy, C.L. Ho, W.Y. Wong, Appl. Phys. Lett. 95 (2009) 133304.
- [17] S. Reineke, G. Schwartz, K. Walzer, K. Leo, Appl. Phys. Lett. 91 (2007) 123508.
- [18] S. Reineke, G. Schwartz, K. Walzer, M. Falke, K. Leo, Appl. Phys. Lett. 94 (2009) 163305.
- [19] F.X. Zang, T.C. Sum, A.C.H. Huan, T.L. Li, W.L. Li, F. Zhu, Appl. Phys. Lett. 93 (2008) 023309.
- [20] M.A. Baldo, M.E. Thompson, S.R. Forrest, Nature 403 (2000) 750.
- [21] B.W. D'Andrade, M.A. Baldo, C. Adachi, J. Brooks, M.E. Thompson, S.R. Forrest, Appl. Phys. Lett. 79 (2001) 1045.
- [22] G.F. He, S.C. Chang, F.C. Chen, Y. Li, Y. Yang, Appl. Phys. Lett. 81 (2002) 1509.
- [23] M. Ichikawa, T. Aoyama, J. Amagai, T. Koyama, Y. Taniguchi, J. Phys. Chem. C 113 (2009) 11520.
- [24] J. Shi, C.W. Tang, Appl. Phys. Lett. 70 (1997) 1665.
- [25] M.A. Baldo, S. Lamansky, P.E. Burrows, M.E. Thompson, S.R. Forrest, Appl. Phys. Lett. 75 (1999) 4.
- [26] F. Li, J. Lin, J. Feng, G. Cheng, H. Liu, S. Liu, L. Zhang, X. Zhang, S.T. Lee, Synth. Met. 139 (2003) 341.